A trilinear method for finding null points in a 3D vector space

A.L. Haynes* and C.E. Parnell

Department of Mathematics and Statistics, University of St Andrews,

North Haugh, St Andrews, KY16 9SS, UK

Abstract

Null points are important locations in vector fields, such as a magnetic field. A new technique (a trilinear method for finding null points) is presented for finding null points over a large grid of points, such as those derived from a numerical experiment. The method was designed so that the null points found would agree with any fieldlines traced using the commonly used trilinear interpolation. It is split into three parts: reduction, analysis and positioning, which, when combined, provide an efficient means of locating null points to a user-defined sub-grid accuracy. We compare the results of the trilinear method with that of a method based on the Poincaré index, and discuss the accuracy and limitations of both methods.

1

I. INTRODUCTION

A null point (or neutral point, 3D root) is a location where the strength of a continuous vector field, such as a magnetic field $(\vec{B})$, is locally zero (i.e. $\vec{B} = \vec{0}$). Null points in magnetic fields are important sites for current sheet formation[1–3], energy dissipation via either magnetic reconnection[4–6] or wave dissipation[7,8]. Furthermore, null points are useful for finding other important topological features[9–13], for example separatrix surfaces and separators. Separatrix surfaces (also known as Σ or fan surfaces) are a set of fieldlines which originate or terminate at a null and divide two topologically distinct regions. Two separatrix surfaces intersect at a separator (or γ line), a special fieldline which connects two null points. Both separatrix surfaces and separators are locations where reconnection preferentially occurs. Examples of magnetic null points have been detected in the laboratory[14] and in the Earth's magnetosphere[15] and they are believed to be important in many astrophysical phenomena such as solar flares and magnetic sub-storms.

In a finite volume, null points may be found in one of two locations: on the boundary or inside the volume. In general, boundary null points may be found using a 2D method on two of the three components, with the third component used to check whether any resulting locations are really null points. Internal null points may exist anywhere within the volume and require a 3D method to locate them. Methods using the Poincaré index such as Greene's[16] work on analytical or numerical fields that are divided into a series of cells. By considering the cell translated in magnetic field space and then mapped onto the unit sphere, their methods deduce if the magnetic field space surrounds a null point. This method can give false positives and false negatives, as discussed in detail later. Furthermore, the null point itself is not actually located, only the grid-cell it is in, unless further assumptions are made, such as multiple iterations for analytical fields or an interpolation approach is chosen for a numerical field. More recently, Zhao[17] has also proposed essentially the same null finding method.

In recent years the use of large computer simulations of magnetic fields has increased, and the output of these experiments is usually as a grid of points, which divide the space into a grid of cells. To analyse this data a fast and accurate null-finding method is required. For fieldlines to be traced within the experimental domain knowledge of the field between the grid points is required. To estimate the field between gridpoints, the field is interpolated, usually

using the method of trilinear interpolation. Although in general this does not conserve $\nabla.\vec{B} = 0$, it is a good first approximation of the magnetic field between grid points. For many situations (e.g. to calculate separatrix surface fieldlines), it is necessary to know exactly where the null points lie to sub-grid resolution.

In this paper, we present a new simple trilinear (TL) method of finding null points that finds the null points of the actual field traced (using trilinear interpolation) to subgrid resolution. We compare our TL method with the commonly used Greene's method identifying the limitations of each method.

First, in Section II we present the linear, bilinear and trilinear equations. Then in Section III the trilinear (TL) method and Greene's method are described. Section IV gives comparative examples of the use of the two methods and Section V describes the limitations of the two methods for linear and non-linear fields. The conclusions (Section VI) gives a brief discussion on the advantages and disadvantages of each method.

II.   INTERPOLATION

A.   Linear, Bilinear and Trilinear Equations

The simplest form of interpolation between $f(0)$ and $f(1)$ in 1D is linear interpolation, which generates an equation of the form:

$$f(x) = f(0) + (f(1) - f(0))x,$$

For simplicity we write

$$f(x) = (1 - x)f_0 + xf_1$$

where $f_0 = f(0)$ and $f_1 = f(1)$.

We expand this to 2D by interpolating linearly along the horizontal sides of a square (of unit length) and then by linear interpolation between the two resulting points. Points along the bottom of the square are given by $p_0(x) = (1 - x)f_{00} + xf_{10}$ and along the top by $p_1(x) = (1 - x)f_{01} + xf_{11}$ (where $f_{00} = f(0,0)$ etc.) Then the field at a point (x, y) is given by interpolating along the vertical line of constant x between points $p_0(x)$ and $p_1(x)$.

Hence,

$$
\begin{aligned}
f(x,y) &= (1-y)p_0(x) + y p_1(x) \\
&= (1-x)(1-y)f_{00} + x(1-y)f_{10} + (1-x)y f_{01} + xy f_{11} \\
&= a + bx + cy + dxy
\end{aligned}
$$

for constants $a = f_{00}$, $b = f_{10} - f_{00}$, $c = f_{01} - f_{00}$ and $d = f_{11} - f_{10} - f_{01} + f_{00}$. Clearly, this gives exactly the same answer if one interpolates first along the vertical edges of the square for constant x and then horizontally for constant y.

Expanding this to 3D, we obtain the trilinear equation for the field at a point (x, y, z) inside a cube of unit length,

$$
f(x,y,z) = a + bx + cy + dxy + ez + fxz + gyz + hxyz. \tag{1}
$$

The values of the constants are unique for each cube, and are found to be:

$$
\begin{aligned}
a &= f_{000}, & b &= f_{100} - f_{000}, \\
c &= f_{010} - f_{000}, & d &= f_{110} - f_{100} - f_{010} + f_{000}, \\
e &= f_{001} - f_{000}, & f &= f_{101} - f_{100} - f_{001} + f_{000}, \\
g &= f_{011} - f_{010} - f_{001} + f_{000}, & h &= f_{111} - f_{110} - f_{101} - f_{011} + f_{100} + f_{010} + f_{001} - f_{000},
\end{aligned}
$$

where $f_{000} = f(0,0,0)$, etc.

These equations form a simple method of interpolation in up to three dimensions and have the property that the values on the shared surface of adjacent cubes are equal. Higher-order methods such as cubic, bicubic and tricubic, are not discussed in this paper.

B. Roots of a pair of bilinear equations.

We will make use of the roots of a pair of bilinear equations later and so discuss how to find their roots here.

For any pair of general bilinear equations

$$
f_i(x,y) = a_i + b_i x + c_i y + d_i xy \tag{2}
$$

with $i \in \{1, 2\}$ the values of x and y which satisfy $f_1(x,y) = f_2(x,y) = 0$ may be found by solving either of the respective quadratic equations

$$
\begin{vmatrix} a_1 & a_2 \\ c_1 & c_2 \end{vmatrix} + \left(\begin{vmatrix} a_1 & a_2 \\ d_1 & d_2 \end{vmatrix} + \begin{vmatrix} b_1 & b_2 \\ c_1 & c_2 \end{vmatrix} \right) x + \begin{vmatrix} b_1 & b_2 \\ d_1 & d_2 \end{vmatrix} x^2 = 0, \tag{3}
$$

or

$$\begin{vmatrix} a_1 & a_2 \\ b_1 & b_2 \end{vmatrix} + \left(\begin{vmatrix} a_1 & a_2 \\ d_1 & d_2 \end{vmatrix} - \begin{vmatrix} b_1 & b_2 \\ c_1 & c_2 \end{vmatrix} \right) y + \begin{vmatrix} c_1 & c_2 \\ d_1 & d_2 \end{vmatrix} y^2 = 0.$$

The resulting 2D coordinate is found using

$$y = -\frac{a_i + b_i x}{c_i + d_i x}, \tag{4}$$

for any known x where $i \in \{1, 2\}$, or using

$$x = -\frac{a_i + c_i y}{b_i + d_i y},$$

for any known y where $i \in \{1, 2\}$.

III. METHODS FOR FINDING NULL POINTS

The trilinear (TL) and Greene's null-finding methods are both split into three distinct parts. The first part, which is the common to both methods, quickly scans over every grid-cell removing most cells which do not contain a null point. The second parts are specific to each method and deduce if a null point does or does not exists inside a flagged grid-cell. The third parts locate the null point within the grid-cell. All three parts of both methods are described below.

Reduction

The first stage of both algorithms is to take every grid-cell and use a simple test to examine whether a null point can exist inside the grid-cell or not. The test assumes that within each cell the field is linear or trilinear. Thus an implicit assumption for both methods is there is adequate resolution in the data. A direct consequence of the trilinear assumption is that it forces the range of values of B_x inside the cell to lie between the minimum and maximum values of B_x at the corners, and similarly for B_y and B_z. Hence, B_x can never be zero inside the cell provided that B_x is non-zero and of the same sign at each corner of the cell.

At each corner of the cell, the signs of the B_x, B_y and B_z are considered in turn. Should any of the three magnetic field components have the same sign at all eight corners of any cell, then that cell is removed from further analysis, as it cannot contain a null point.

A.   Trilinear Method

The analysis part of the TL method is based upon the fact that a null point, if it exists, must lie on all three of the following curves: $B_x = B_y = 0$, $B_x = B_z = 0$ and $B_y = B_z = 0$. These curves must be one of two types: (i) a circuit inside a cell or (ii) a curve that extends through the boundary of the cell at either end. The first case equates to having two null points within a cell. This implies considerable sub-grid structure and clearly shows insufficient grid resolution, as does Greene[16]. The second case is the most important, and the TL algorithm is designed to detect these types of null points.

On the surface of the cell the lines $B_x = 0$, $B_y = 0$ and $B_z = 0$ are found. Clearly, due to the trilinear nature inside the cell, B_x, B_y and B_z are bilinear on each face of the cell. This allows us to use the analytical solution presented in Section II B, for any pair of bilinear equations, to find all intersections of each of the three pairs of lines $B_x = 0$, $B_y = 0$ and $B_z = 0$ on all faces of the cell. These intersections represent all locations where any of the intersection curves (e.g. $B_x = B_y = 0$) cross the boundary of the cell.

In general, each of these intersection curves must pierce the boundary of the cell in pairs. Indeed, this is a necessary condition for a single null point to exist along any such intersection curve. However, it is possible that there may be more than one pair of points where the intersection curves cross the cell boundary. A null point only exists if given any single intersection curve inside the boundary, with a pair of end points on the boundary, the third component is of opposite sign at the end points.

Once the existence of a null point has been deduced within a given cell, we then locate its position to subgrid resolution. There are many possible methods to do this. We have found the following Newton-Raphson method fast and generally successful.

A 3D version of the iterative Newton-Raphson method for finding roots of equations has the step:

$$\vec{x_{n+1}} = \vec{x_n} - \left[\nabla \vec{B} \Big|_{\vec{x_n}} \right]^{-1} \vec{B}(\vec{x_n}) \tag{5}$$

where

$$\left[\nabla \vec{B} \right]_{ij} = \frac{\partial B_i}{\partial x_j}.$$

This is repeated until $|\vec{x_{n+1}} - \vec{x_n}|$ or $|\vec{B}(\vec{x_n})|$ is less than a given tolerance. When the trilinear assumption is used, the differentials can be explicitly written in terms of the components of

$\vec{x}$, and we choose $\vec{x_0}$ to be at either the centre of the cell or a cell corner. Various starting points are tried until the iterative method succeeds at some point within the cell. If this method fails we split the grid-cell into eight subgrid-cells using trilinear interpolation and use the TL method again on these eight new cells.

As an aside it is clear that this method may also be implemented for any 2D field (say when $B_z = 0$). By using the fast scanning method described in the first part of the algorithm on the four points around a grid-square for B_x and B_y only, we remove many locations where a 2D null point cannot exist. The locations of any null points in this 2D field is then found by solving the pair of bilinear equations (in B_x and B_y) derived from the values of the magnetic field at the corners.

B. Greene's method

Greene[16] proposed a method based on the Poincaré index theorem to determine the existence of a null point within a given cell. We give a brief description here for completeness.

The analysis part of the algorithm, determines the existence of a null point within a grid-cell. Each of the six rectangular faces which make up the boundary of the cell is divided into two triangles, of which there are two choices (a point which shall be important later). For each triangle, the positions of the three magnetic field vectors $\vec{B_1}$, $\vec{B_2}$ and $\vec{B_3}$ are ordered in a right-handed manner about the normal vector of the cell. From this the *area contribution* (A) of the triangle, is calculated from

$$\tan^2 \frac{A}{4} = \tan \frac{\theta_1 + \theta_2 + \theta_3}{4} \tan \frac{\theta_1 + \theta_2 - \theta_3}{4} \tan \frac{\theta_2 + \theta_3 - \theta_1}{4} \tan \frac{\theta_3 + \theta_1 - \theta_2}{4}, \quad (6)$$

and

$$\cos\theta_1 = \frac{\vec{B_2}.\vec{B_3}}{|\vec{B_2}||\vec{B_3}|}, \qquad \cos\theta_2 = \frac{\vec{B_1}.\vec{B_3}}{|\vec{B_1}||\vec{B_3}|}, \qquad \cos\theta_3 = \frac{\vec{B_1}.\vec{B_2}}{|\vec{B_1}||\vec{B_2}|}.$$

Finally the area contribution, A, is chosen to be negative if $\vec{B_1}.\vec{B_2} \times \vec{B_3}$ is negative, else the area contribution is taken to be positive. The deviation of these area contributions is trivial to show using spherical geometry techniques.

The topological degree of the cell is determined by summing up all twelve area contributions, and then dividing the result by 4π. The cell contains a null point if the topological degree is non-zero (a positive null if the degree is -1, a negative null if $+1$).

Further refinement is given by bisecting the cell to gain greater accuracy. Greene[16] also implemented a method of guessing the location of a null point near the point $\vec{x}_0 = \langle x_0, y_0, z_0 \rangle$ (the secant method) by solving the three simultaneous equations

$$\frac{\vec{B}_x - \vec{B}_0}{\delta x}(x - x_0) + \frac{\vec{B}_y - \vec{B}_0}{\delta y}(y - y_0)\frac{\vec{B}_z - \vec{B}_0}{\delta z}(z - z_0) = -\vec{B}_0, \tag{7}$$

for x, y and z, where $\vec{B}_0 = \vec{B}(\vec{x}_0)$, $\vec{B}_x = \vec{B}(\vec{x}_0 + \delta x\, \hat{x})$, $\vec{B}_y = \vec{B}(\vec{x}_0 + \delta y\, \hat{y})$ and $\vec{B}_z = \vec{B}(\vec{x}_0 + \delta z\, \hat{z})$, and δx, δy and δz are small. This approach is similar to the Newton-Raphson method which was described earlier.

IV.   EXAMPLES COMPARING METHODS

To demonstrate the differences between the TL and Greene's method, we consider a couple of examples.

A.   Example I

The speed and accuracy of the null-finding methods is tested on a frame of a numerical experiment involving a twisted flux tube rising through another twisted flux tube beneath the solar photosphere[18]. Both the TL method and Greene's method positively identified the same six grid-cells containing null points in the frame (see Figure 1).

The TL method took just 24.9 seconds to do this compared to Greene's 25.0 seconds, hence the algorithms operate at comparable speeds. The reduction phase reduced the number of grid-cells to search from 581433 to 781 (a reduction of 99.87%).

B.   Example II

The accuracy of the TL method and Greene's test were compared using a sample frame of a simulation of the Earth's magnetosphere[19]. Both methods returned the same eight null points, but Greene's test found another two possible null points and the TL method found a further six (see Figure 2). Clearly in a numerical experiment it is not possible to know exactly what the field inside the cells without rerunning the experiment at higher resolution, which is rarely practical. However, if we assume the field to be trilinear within each cell, it

FIG. 1: (Color Online) Example showing the null points found by both null-finding methods on a sample frame of a numerical experiment[18] involving two twisted flux tubes passing through one another. Both methods found six null points (shown as spheres) between the two flux tubes, which are shown as sets of fieldlines traced from the sides of the box.

is possible to show that Greene's extra "nulls" are false positives and that TL's extra nulls are actual null points. In the next section, we shall discuss the accuracy of both techniques, with respect to analytic types of field.

V.   DISCUSSION OF ACCURACY OF METHODS

A.   Linear Fields

All linear fields can be written in the form

$$\vec{B}(\vec{x}) = \vec{a}x + \vec{b}y + \vec{c}z + \vec{d} = \begin{bmatrix} \vec{a} & \vec{b} & \vec{c} \end{bmatrix} \vec{x} + \vec{d}, \tag{8}$$

where $\vec{a}$, $\vec{b}$, $\vec{c}$ and $\vec{d}$ are arbitrary constant vectors of the form $\vec{a} = \langle a_1, a_2, a_3 \rangle$. Provided the matrix $[\nabla \vec{B}] = [\vec{a} \ \vec{b} \ \vec{c}]$ is non-singular (which is the case for a generic 3D field), this can be rewritten as $\vec{B}(\vec{x}) = [\nabla \vec{B}](\vec{x} - \vec{x}_N)$, where $\vec{x}_N = -[\nabla \vec{B}]^{-1}\vec{d}$.
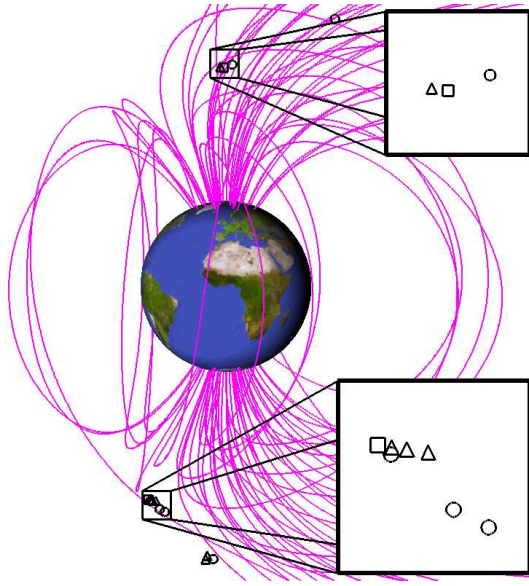
FIG. 2: (Color Online) A sample frame of the Earth's magnetospheric magnetic field[19] used to compare the null finding codes. The small symbols represent points identified as nulls (triangle – TL method, square – Greene's test, circle – both TL method and Greene's test). Note that two distant null points found by both methods are not shown. The lines represent sample fieldlines traced from the poles of the Earth.

1. Greene's Method

To demonstrate that Greene's method will always correctly identify null points in a linear field, we need only consider the signs of the triangular area contributions (A), which are each given by the triple scalar product $\chi(\triangle PQR) = \vec{B}(\vec{P}) \cdot \vec{B}(\vec{Q}) \times \vec{B}(\vec{R})$ for triangle $\triangle PQR$. Hence,

$$
\begin{aligned}
\chi(\triangle PQR) &= \vec{B}(\vec{P}) \cdot \vec{B}(\vec{Q}) \times \vec{B}(\vec{R}) \\
&= \left\{ \left[\nabla \vec{B} \right] (\vec{P} - \vec{x}_N) \right\} \cdot \left\{ \left[\nabla \vec{B} \right] (\vec{Q} - \vec{x}_N) \right\} \times \left\{ \left[\nabla \vec{B} \right] (\vec{R} - \vec{x}_N) \right\} \\
&= \left| \nabla \vec{B} \right| \left(\left\{ \vec{P} - \vec{x}_N \right\} \cdot \left\{ \vec{Q} - \vec{x}_N \right\} \times \left\{ \vec{R} - \vec{x}_N \right\} \right)
\end{aligned}
\tag{9}
$$

Clearly $|\nabla \vec{B}|$ is constant and hence of fixed sign throughout the domain. So if we determine χ for all triangles in a right-handed manner relative to the outwards normal vector of the volume enclosed by the triangles then, if there is a null point inside this volume, the sign for each χ will be the same. If positive there is a negative null point inside the volume, if

negative a positive null point. In particular, note that the sign of both triangles on any one face of a cell will be the same. Hence, Greene's method will always find a null point if one exists within the volume. If the null point is outside the cell, the triangles relative to $\vec{x}_N$ have χ of mixed sign.

Clearly, if a null point exists within a cell then the topological degree is either ± 1. For any linear field containing a null point, it is possible to choose cells of any size and still resolve the field within the cell. This lets us consider a large cell that contains a null point. This large cell may be divided in to a grid of n smaller cells, of which $n-1$ do not contain a null point. The topological degree of this big cell must be the sum of the topological degrees of the smaller cells which span it. Furthermore, we note that the topological degrees for the large cell and the small cell containing the null point are 1 (assuming we have a negative null point, without loss of generality). Thus, by considering the case of $n = 2$ and working up, it is clear that the topological degree of all smaller cells without a null point may be deduced to be zero. Therefore, the topological degree determined by Greene's method will always be correct for any cell in a linear field.

2. Trilinear Method

Similarly we can show that the TL method also always correctly identifies a null point in a linear field. If we consider the surface $\langle a_1, b_1, c_1 \rangle \,.\vec{x} = -d_1$, where $B_x = 0$, and the surface $\langle a_2, b_2, c_2 \rangle \,.\vec{x} = -d_2$, where $B_y = 0$, then their intersection will be a straight line in the direction $\vec{n} = \langle a_1, b_1, c_1 \rangle \times \langle a_2, b_2, c_2 \rangle$, and the line will be of the form $\vec{x}(s) = \vec{x}_0 + \vec{n}s$, where $\vec{x}_0$ is any point on both planes. An obvious choice for this point is the null point, $\vec{x}_N$, hence $\vec{x}(s) = \vec{n}s - \begin{bmatrix} \vec{a} & \vec{b} & \vec{c} \end{bmatrix}^{-1} \vec{d}$. Calculating $\vec{B}$ along this line, we find

$$
\begin{aligned}
\vec{B}(s) &= \begin{bmatrix} \vec{a} & \vec{b} & \vec{c} \end{bmatrix} \left\{ \vec{n}s - \begin{bmatrix} \vec{a} & \vec{b} & \vec{c} \end{bmatrix}^{-1} \vec{d} \right\} + \vec{d} \\
&= \begin{bmatrix} \vec{a} & \vec{b} & \vec{c} \end{bmatrix} (\langle a_1, b_1, c_1 \rangle \times \langle a_2, b_2, c_2 \rangle \, s) - \vec{d} + \vec{d} \\
&= \left| \begin{bmatrix} \vec{a} & \vec{b} & \vec{c} \end{bmatrix} \right| s\hat{\vec{z}}.
\end{aligned}
\tag{10}
$$

From this it is obvious that B_z does not change sign along its length except at the null point (when $s = 0$).

We have a two cases:

1. Part of the line is inside the cell: Since the line is straight and of infinite length, then for any finite volume which the line passes through, the line intersects the surface at least twice. The TL method detects these locations. Since the sign of B_z changes only at the single null on this line, the null point must be inside the cell if, and only if, the sign of B_z is different at the locations where it intersects the surface of the cell. Thus this agrees with the TL method.

2. None of the line is inside the cell: Since the (only) null point is on this line, it cannot be inside the cell. As the TL method does not detect this line on the surface of the cell, it rightly returns that no null exists within the cell.

This above argument holds for all pairings of field components. Furthermore, since the field is linear, the final positioning part will succeed after the first step, as the iterative step,

$$\vec{x}_{i+1} = \vec{x}_i - \left[\nabla\vec{B}\right]^{-1}\vec{B}(\vec{x}_i) = \vec{x}_i - \left[\begin{array}{ccc}\vec{a} & \vec{b} & \vec{c}\end{array}\right]^{-1}\left(\left[\begin{array}{ccc}\vec{a} & \vec{b} & \vec{c}\end{array}\right]\vec{x}_i + \vec{d}\right) = -\left[\begin{array}{ccc}\vec{a} & \vec{b} & \vec{c}\end{array}\right]^{-1}\vec{d} = \vec{x}_N,$$

(11)

for any value of $\vec{x}_i$.

B. Nonlinear Fields

Nonlinear fields are clearly more complicated than linear fields and this is where the results from the two methods can diverge.

1. Greene's Method

We return to the results of Example II, where we have noted discrepancies between the results of Greene's method and the TL method. By swapping the choice of triangles for each face of the grid-cells for Greene's method, we find fourteen null points with this alternative implementation. Six are new, four the same as those found previously by the TL method alone and a further four are the same as four found previously by both the TL method and the original Greene's implementation. This leads to a curious result about the nature of Greene's method when implemented for non-linear fields.

It is known that the sum of all the area contributions in Greene's method must sum up to an integer, and the triangles chosen for each face may be changed independently from the

other faces. If the result of Greene's algorithm changes depending on the choice of triangles, then the difference between the area contributions using one choice of triangles on the face must be an integer difference to the other choices. Using Example II, we found that different implementations of Greene's method could add or remove a null point, or even (in a few cases) change the sign of the null point.

To further this investigation, we analysed a set of trilinear fields where the solenoidal condition $(\nabla.\vec{B} = 0)$ was satisfied. This choice of non-linear field is chosen because the field inside numerical cells is typically assumed to be trilinear and because the TL method can easily find these null points. Numerous fields were found (using a method described in Appendix A) where at least one of the faces of a cell would change the topological degree in the cell depending on the choice of triangles producing both false negatives and false positives. Although most of the cases involved the null point existing near the face in question, some cases were found where null points were near the grid-cell's centre.

An example trilinear field is given below which contains two null points and demonstrates the curious behaviour of Greene's method under different implementations.

$$\vec{B}(\vec{x}) = \begin{pmatrix} -1.80 \\ 0.44 \\ -0.67 \end{pmatrix} + \begin{pmatrix} -2.57 & 6.92 & 0.44 \\ -3.05 & 2.09 & 0.20 \\ -2.30 & 8.69 & 0.48 \end{pmatrix} \begin{pmatrix} x \\ y \\ z \end{pmatrix} + \begin{pmatrix} 0.02 & 0.46 & -1.40 \\ -0.46 & -0.34 & 1.46 \\ 1.40 & -1.46 & -8.29 \end{pmatrix} \begin{pmatrix} yz \\ xz \\ xy \end{pmatrix}. \quad (12)$$

In this example field, we have a negative null point at $(0.59, 0.49, 0.44)$ and a positive null point at $(0.23, 0.11, 3.23)$. In the cell $[0, 1]^2 \times [-1, 0]$ which contains no null point, Greene's algorithm gives the topological degree to be -1 or 0 depending on how the face $z = 0$ is divided (see Figure 3). We now extend our region of interest to the sequential group of cells $[0, 1]^2 \times [-1, 0]$, $[0, 1]^3$, $[0, 1]^2 \times [1, 2]$, $[0, 1]^2 \times [2, 3]$ and $[0, 1]^2 \times [3, 4]$. In this case we have four internal faces between the cells. If we consider only implementations of Greene's method where the triangles coincide on these faces, of which there are sixteen, each yields a different result: one with no null points in any cell (i.e. topological degree of the cells is $(0, 0, 0, 0, 0)$ for increasing z), ten results detect one positive and one negative null point (e.g. $(-1, 1, 0, 0, 0)$, $(-1, 0, 1, 0, 0)$, $(0, 0, -1, 0, 1)$ where order must be -1 then 1 ignoring zeros – note one of these is the correct solution $(0, -1, 0, 0, 1)$) and five with two positive and two negative null points (e.g. $(-1, 1, 0, -1, 1)$, again in order -1, 1, -1, 1 with the 0 in any one of the five cells). Thus, Greene's method may (i) move null points a significant distance or
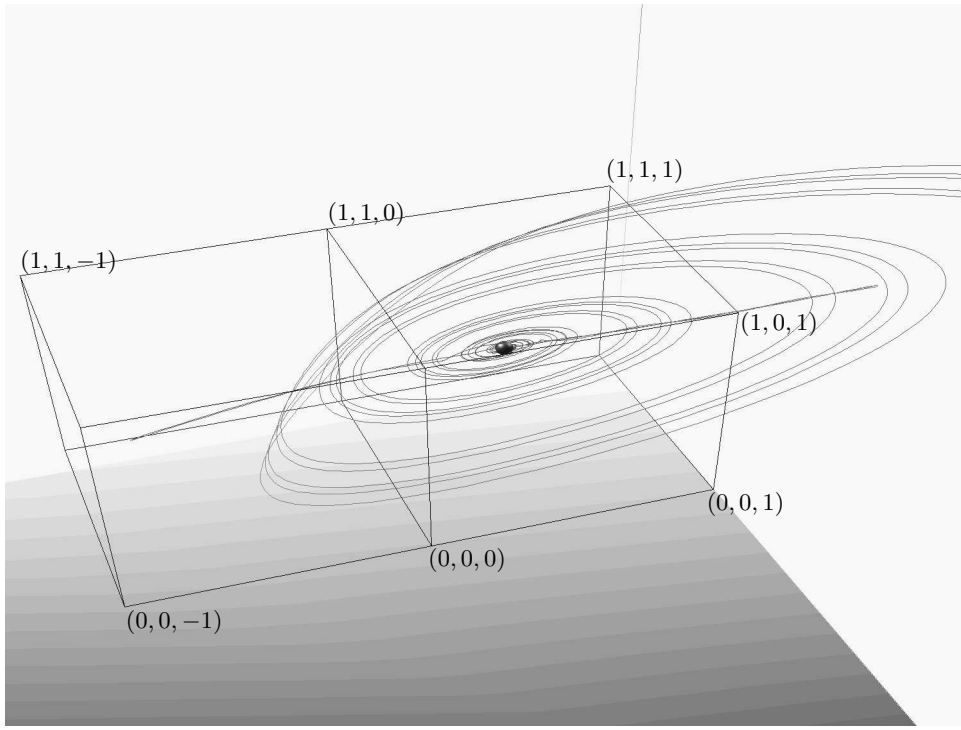
FIG. 3: Fieldlines showing the spines and separatrix surfaces of the null point in the trilinear field given by Equation 12 where Greene[16] may fail upon implementation. The $z = 0$ face which changes the topological degree in the left cell from -1 to 0 is the one between the two cells drawn.

(ii) change the number of null points. Furthermore it is not possible to say which of the above implementations of Greene's method is correct without either prior knowledge of the result or increasing the resolution of the grid. In an analytical field case, bisecting over the complete region will generally reduce the likelihood of such a failure, but on a numerical grid this would require assumptions about the magnetic field within the domain.

In this example the ratio of the maximum absolute value of the nonlinear terms to the linear terms is 0.95, showing significant nonlinearity. But significant nonlinearity is not essential for Greene's method to give a false reading, as Example II includes a number of cases where the ratio in such cases is lower than 0.25.

Note in the above example we always choose the triangles on the internal cell faces to coincide for both cells on either side of the face. Thus in swapping the choice of triangles (for both grid-cells), we can only add or remove null points in opposite polarity pairs or move the existing null point between grid-cells leaving the overall topological degree of the

14

region unchanged. Should the triangles of only one of these two cells on either side of the face change, then this cell could create or destroy a single null point. Hence, it is important that when implementing Greene's method, the triangles of all internal faces are chosen to coincide.

2. Trilinear Method

We now discuss the accuracy of the TL method. First, we shall look at the nature of trilinear fields, followed by a discussion of the accuracy for a general non-linear field.

Trilinear fields have four non-linear terms (xy, xz, yz and xyz), and are solvable using the TL method. An important point to note though about trilinear fields is that they are not rotationally preserved, e.g. if we take the function $f(x, y, z) = 1 + xy$, and rotate it by $45°$ about $\hat{\bar{z}}$ then we obtain the function

$$F(X, Y, Z) = f\left(\frac{X - Y}{\sqrt{2}}, \frac{X + Y}{\sqrt{2}}, Z\right) = 1 + \frac{X^2 - Y^2}{2},$$

where $F(X, Y, Z)$ is the function in the rotated space X, Y, Z, which is obviously not trilinear. Hence, if we rotate a grid by any angle, the exact results of the TL method may vary. Since the TL method only locally approximates the field as trilinear, it may still be used to locate the null point in the rotated field.

If we relax the conditions to a general non-linear field, it is possible using the TL method for a null point to be found in a different cell if the field is sufficiently non-linear. As a null point exists on the intersection of a line ($B_x = B_y = 0$, say) and a surface ($B_z = 0$, say), and both of these are either closed or extend through the boundary of the full domain, null points can only be removed or added in pairs within the domain, or singularly though the boundary of the full domain. If we consider that a null point is at the intersection of the three surfaces ($B_x = 0$, $B_y = 0$ and $B_z = 0$) and hence at the corner of the eight volumes bounded by these three surfaces. This null point may only be removed if any of these eight volumes is removed. Provided the grid is fine enough, then there should exist a grid point within each volume bounded by the three surfaces. Since the grid point has a known field, it must stay within the same volume, and hence the volume cannot be destroyed, even if the resulting trilinear field is vastly different from the real field. Thus, no null points can disappear for the TL method (although its position may vary) if this condition is satisfied.

We clarify this with a 2D example.

If the above argument is considered in 2D, the surfaces ($B_x = 0$, etc.) become lines and the volumes bounded by the surfaces become areas bounded by lines. An example grid with $B_x = 0$ and $B_y = 0$ is shown on the left of Figure 4. For a null point to be found in 2D, the TL method looks for intersections of the lines $B_x = 0$ and $B_y = 0$. Since the TL method assumes the field within four grid points to be bilinear, these lines may be deformed from the real field. However, the real field is known at each grid point, so the lines $B_x = 0$, etc. found must pass through the same edge as the real lines $B_x = 0$, etc., since otherwise the sign of B_x, etc. at the grid points would change. Should a grid point exist within each area bounded by zero lines, for example area C which contains grid point G, (in the left part of Figure 4), the area may be deformed, but can never be removed by any continuous interpolation of the field, since grid point (G) can only exist within this area. Hence, the null points (A and B) must always be preserved. In the case of an area with no grid point within it, for example area γ (in the right part of Figure 4), the area may be deformed and shrunk by a continuous interpolation of the field until the null points α and β meet and are annihilated, as the areas δ and ε merge. In this case, pairs of null points may be lost (or added by the converse argument) by the TL method. In this example, if the field is locally close to linear or trilinear, the approximation of the intersection of the lines ($B_x = 0$ and $B_y = 0$) to the line between the grid points ζ_1 and ζ_2 will be roughly correct and the TL method will still find the null points even with no grid point in area γ. For false readings in the TL method to occur, the field must be very highly nonlinear, and hence severely under-resolved.

VI. CONCLUSION

It is well known that the location of null points is important in the understanding of magnetic topology and for some types of reconnection and wave dissipation. Here, we have presented a new technique, the trilinear (TL) method, for finding null points in a magnetic field, in particular for whose field is calculated using numerical code. The TL method includes three stages. A reduction stage to quickly remove most grid-cells which do not contain a null point. An analysis to positively identify cells containing a null point using the bilinear nature of the field on the boundaries, and finally a stage to determine the exact location of the null point according to trilinear interpolation.
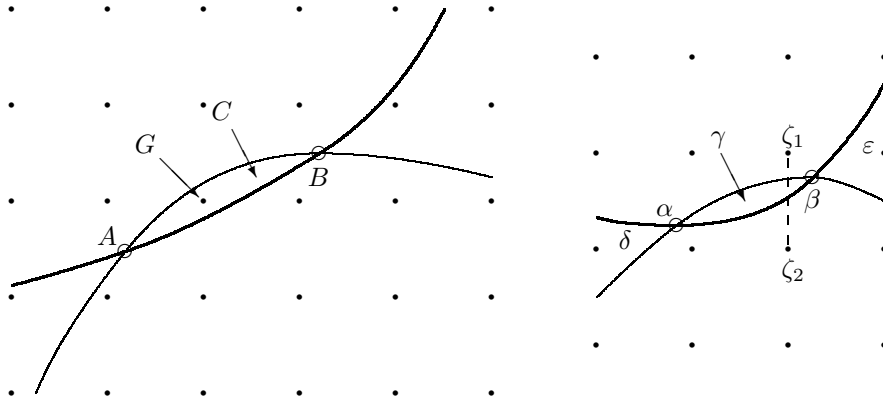
FIG. 4: Left: Example configuration of the TL method which cannot lose a null point. The thick line denotes $B_x = 0$, the thin line $B_y = 0$ and the hollow circles (A and B) represent null points. The dots represent the grid used in the TL method. C refers to the area between the null points bounded by the thick and thin lines. Right: Example configuration of the TL method which may lose a null point for nonlinear fields. The thick line denotes $B_x = 0$, the thin line $B_y = 0$ and the hollow circles (α and β) represent null points. The dots represent the grid used in the TL method. γ, δ and ε refer to the area bounded by the thick and thin lines.

We compare our TL method with the Poincaré index based method of Greene[16]. Both the TL and Greene's method are accurate for all linear fields. The TL method is in general accurate for most nonlinear fields. Null points may be falsely created or destroyed, either in pairs or lost through the boundary of the domain where the field within a cell is highly nonlinear. If we restrict the field to being trilinear within cells, the TL method is accurate except when two null points exist within one cell making it highly suitable for numerical magnetic fields.

Greene's method has similar failings to the TL method. In Greene's method the choice of triangles on the cell faces is arbitrary. In certain (moderately as well as highly) non-linear fields different implementations of Greene's algorithm, assuming a different choice of triangles, give rise to failings in the method. If triangles on internal faces are kept coincident, null points can only be lost in pairs from inside the domain (or singularly through the boundary). However, if the triangles on internal faces are not kept coincident then null points may be created and destroyed singularly from anywhere within the domain. A single implementation of Greene's method should not be used on its own as it is not clear how many or where the null points should be. A result can only be relied upon if all coincident triangle

implementations agree. By using different implementations of Greene's method it is possible to detect where Green's method is failing, but this does not help give the correct answer unless the resolution of the grid can be increased. However, Greene's algorithm is very useful for finding null points in analytical fields, whilst the TL method is most applicable for numerical fields.

APPENDIX A: FAILURE OF GREENE'S ALGORITHM

A means to finding a cell where Greene's algorithm fails is as follows. Looking at a face of a cell, say $z = 0$ with $x, y \in [0, 1]$, the magnetic field vectors are $\vec{B}_{000}$, $\vec{B}_{100}$, $\vec{B}_{010}$ and $\vec{B}_{110}$ at the corners. On our face, we wish to have each pair of triangular area contributions to have opposite sign. So, for instance, the triple scalar products of the magnetic field vectors in the corners may satisfy

$$
\begin{aligned}
\vec{B}_{000}.\vec{B}_{100} \times \vec{B}_{110} &> 0, & \vec{B}_{000}.\vec{B}_{110} \times \vec{B}_{010} &> 0, \\
\vec{B}_{000}.\vec{B}_{100} \times \vec{B}_{010} &< 0, & \vec{B}_{100}.\vec{B}_{110} \times \vec{B}_{010} &< 0,
\end{aligned}
\tag{A1}
$$

or have all inequalities reversed. Since multiplying any vector by a positive constant does not change the sign of the triple vector product, we shall assume all vectors are normalised. Let us then choose an invertible matrix T, which satisfies the following three properties:

$$
T\vec{x} = \vec{B}_{000}, \qquad T \begin{pmatrix} \cos\theta_1 \\ \sin\theta_1 \\ 0 \end{pmatrix} = \vec{B}_{100}, \qquad |T| = 1
\tag{A2}
$$

18

for some θ_1. From this we find a θ_2, θ_3, ϕ_2 and ϕ_3 such that

$$T \begin{pmatrix} \cos\theta_2 \cos\phi_2 \\ \sin\theta_2 \cos\phi_2 \\ \sin\phi_2 \end{pmatrix} = \vec{B}_{010}, \qquad T \begin{pmatrix} \cos\theta_3 \cos\phi_3 \\ \sin\theta_3 \cos\phi_3 \\ \sin\phi_3 \end{pmatrix} = \vec{B}_{110}. \qquad (A3)$$

Thus our inequalities become

$$\begin{vmatrix} 1 & \cos\theta_1 & \cos\theta_2 \cos\phi_2 \\ 0 & \sin\theta_1 & \sin\theta_2 \cos\phi_2 \\ 0 & 0 & \sin\phi_2 \end{vmatrix} > 0, \qquad \begin{vmatrix} 1 & \cos\theta_2 \cos\phi_2 & \cos\theta_3 \cos\phi_3 \\ 0 & \sin\theta_2 \cos\phi_2 & \sin\theta_3 \cos\phi_3 \\ 0 & \sin\phi_2 & \sin\phi_3 \end{vmatrix} > 0,$$

$$\begin{vmatrix} 1 & \cos\theta_1 & \cos\theta_3 \cos\phi_3 \\ 0 & \sin\theta_1 & \sin\theta_3 \cos\phi_3 \\ 0 & 0 & \sin\phi_3 \end{vmatrix} < 0, \qquad \begin{vmatrix} \cos\theta_1 & \cos\theta_2 \cos\phi_2 & \cos\theta_3 \cos\phi_3 \\ \sin\theta_1 & \sin\theta_2 \cos\phi_2 & \sin\theta_3 \cos\phi_3 \\ 0 & \sin\phi_2 & \sin\phi_3 \end{vmatrix} < 0.$$

From these we deduce that

$$\sin\theta_1 \sin\phi_2 > 0, \qquad\qquad \sin\theta_2 \cos\phi_2 \sin\phi_3 > \sin\theta_3 \cos\phi_3 \sin\phi_2,$$

$$\sin\theta_1 \sin\phi_3 < 0, \qquad \cos\phi_2 \sin\phi_3 \begin{vmatrix} \cos\theta_1 & \cos\theta_2 \\ \sin\theta_1 & \sin\theta_2 \end{vmatrix} < \sin\phi_2 \cos\phi_3 \begin{vmatrix} \cos\theta_1 & \cos\theta_3 \\ \sin\theta_1 & \sin\theta_3 \end{vmatrix}. \qquad (A4)$$

Now, let $\alpha = \tan\phi_2 / \tan\phi_3$ so that the last two inequalities become

$$\sin\theta_2 > \alpha \sin\theta_3, \qquad \sin(\theta_2 - \theta_1) < \alpha \sin(\theta_3 - \theta_1), \qquad (A5)$$

provided that $\cos\phi_2 \sin\phi_3 > 0$, otherwise the inequalities are reversed. Now we may choose any value for α and θ_1, then find values for θ_2 and θ_3 so that either pair of the above equalities hold, and choose a Φ_2 and Φ_3 which satisfy $\alpha = \tan\Phi_2 / \tan\Phi_3$. To satisfy the final conditions, let ϕ_2 and ϕ_3 be given from this table:

$\cos\Phi_2 \sin\Phi_3$	$\sin\theta_1 \sin\Phi_2 > 0$ $\sin\theta_1 \sin\Phi_3 < 0$	$\sin\theta_1 \sin\Phi_2 > 0$ $\sin\theta_1 \sin\Phi_3 > 0$	$\sin\theta_1 \sin\Phi_2 < 0$ $\sin\theta_1 \sin\Phi_3 < 0$	$\sin\theta_1 \sin\Phi_2 < 0$ $\sin\theta_1 \sin\Phi_3 > 0$
> 0	$\phi_2 = \Phi_2$ $\phi_3 = \Phi_3$	$\phi_2 = \pi - \Phi_2$ $\phi_3 = -\Phi_3$	$\phi_2 = -\Phi_2$ $\phi_3 = \pi - \Phi_3$	$\phi_2 = \Phi_2 - \pi$ $\phi_3 = \Phi_3 - \pi$
< 0	$\phi_2 = \pi - \Phi_2$ $\phi_3 = \pi - \Phi_3$	$\phi_2 = \Phi_2$ $\phi_3 = \Phi_3 - \pi$	$\phi_2 = \Phi_2 - \pi$ $\phi_3 = \Phi_3$	$\phi_2 = -\Phi_2$ $\phi_3 = -\Phi_3$

19

Thus, provided θ_2 and θ_3 can be found, a field can be generated by taking the subsequently found ϕ_2 and ϕ_3 and creating the four corner vectors of the face. These vectors are then transformed through the transformation matrix T to allow for more generality in the direction of the field. Following this, positive constants can multiply the resulting corner vectors, so they have any required magnitude. From these four vectors, a trilinear field may be extrapolated, with the condition $\nabla . \vec{B} = 0$ satisfied, using

$$
\vec{B}(\vec{x}) = \begin{pmatrix} a_1 \\ a_2 \\ a_3 \end{pmatrix} + \begin{pmatrix} b_1 & c_1 & \alpha \\ a_2 & c_2 & \beta \\ a_3 & c_3 & -(b_1 + c_2) \end{pmatrix} \begin{pmatrix} x \\ y \\ z \end{pmatrix} + \begin{pmatrix} \varepsilon & \gamma & d_1 \\ -\gamma & \delta & d_2 \\ -d_1 & -d_2 & d_3 \end{pmatrix} \begin{pmatrix} yz \\ xz \\ xy \end{pmatrix}, \qquad (A6)
$$

where α, β, γ, δ and ε are arbitrary constants, and

$$
\begin{aligned}
\langle a_1, a_2, a_3 \rangle &= \vec{B}_{000}, & \langle b_1, a_2, b_3 \rangle &= \vec{B}_{100} - \vec{B}_{000}, \\
\langle c_1, a_2, c_3 \rangle &= \vec{B}_{010} - \vec{B}_{000}, & \langle d_1, a_2, d_3 \rangle &= \vec{B}_{110} - \vec{B}_{100} - \vec{B}_{010} + \vec{B}_{000}.
\end{aligned}
$$

---

[*] Electronic address: andrew@mcs.st-andrews.ac.uk

[1] R.M. Green, Stellar and Solar Magnetic Fields, Proceedings of the International Astronomical Union Symposium No. 22., München, 1963 (North-Holland Pub. Co., Amsterdam, 1965) p. 398.

[2] S.I. Syrovatsky, Annual Review of Astron. Astrophys. **19** 121 (1981).

[3] D.I. Pontin, A. Bhattacharjee, K. Galsgaard, "Current sheet formation and non-ideal behaviour at three-dimensional magnetic null points," submitted to Phys. Plasmas.

[4] E.R. Priest, V. Titov, Phil. Trans. Roy. Soc. Lond. **355** 2951 (1996).

[5] D.I. Pontin, G. Hornig, E.R. Priest, Geophys. Astrophys. Fluid Dyn. **98** 407 (2004).

[6] D.I. Pontin, I.J.D. Craig, Phys. Plasmas **12** 072112 (2005).

[7] J.A. McLaughlin, A.W. Hood, Astron. Astrophys. **435** 313 (2005)

[8] J.A. McLaughlin, A.W. Hood, Astron. Astrophys. **459** 641 (2006).

[9] T.N. Bungey, V.S. Titov, E.R. Priest, Astron. Astrophys. **308** 233 (1996).

[10] E.R. Priest, T. Bungey, V. Titov, Geophys. Astrophys. Fluid Dyn. **84** 127 (1997).

[11] C.J. Schrijver, A.M. Title, Solar Phys. **207** 223 (2002).

[12] D.S. Cai, K. Nishikawa, B. Lembege, Plasma Phys. Controlled Fusion **48** B123 (2006).

[13] C.E. Parnell, J.M. Smith, T. Neukirch, E.R. Priest, Phys. Plasmas **3** 759 (1996).

[14] R.L. Stenzel, J.M. Urrutia, M. Griskey, K. Strohmaier, Phys. Plasmas **9** 1925-1930 (2002).

[15] C.J. Xiao, X.G. Wang, Z.Y. Pu, *et al.*, Nature Phys., **2** 478 (2006).

[16] J.M. Greene, J. Comput. Phys. **98** 194 (1992).

[17] H. Zhao J-X. Wang, J. Zhang, C-J. Xiao, Chin. J. Astron. Astrophys. **5** 443 (2005).

[18] M.J. Murray, A.W. Hood, "Simple Emergence Structures from Complex Magnetic Fields", submitted to Astron. Astrophys.

[19] J.C. Dorelli, A. Bhattacharjee, J. Raeder, J. Geophys. Res. **112** A02202 (2007).